

Increase of dissolved inorganic carbon and decrease of pH in near surface waters of the Mediterranean Sea during the past two decades

Liliane. Merlivat ^a, Jacqueline. Boutin ^a, David. Antoine ^{b,c}, Laurence. Beaumont ^d, Melek. Golbol ^b, Vincenzo. Vellucci. ^b

^a Sorbonne Universités (UPMC, Univ Paris 06)-CNRS-IRD-MNHN, LOCEAN Laboratory, F-75005 Paris, France

^b Sorbonne Universités (UPMC, Univ Paris 06)-CNRS, LOV, Observatoire Océanologique, Villefranche-sur-Mer 06230, France

^c Remote Sensing and Satellite Research Group, Department of Physics and Astronomy, Curtin University, Perth, WA 6845, Australia

^d Division Technique INSU-CNRS, 92195 Meudon Cedex, France

Corresponding author: L. Merlivat (merlivat@locean.upmc.fr)

Abstract

Two three-year-long time series of hourly measurements of the fugacity of CO₂ (fCO₂) in the upper 10m of the surface layer of the northwestern Mediterranean Sea have been recorded by CARIOCA sensors almost two decades apart, in 1995-1997 and 2013-2015. By combining them with alkalinity derived from measured temperature and salinity, we calculate changes of pH and dissolved inorganic carbon (DIC). DIC increased in surface seawater by ~ 25 μmol kg⁻¹ and fCO₂ by 40 μatm, whereas seawater pH decreased by ~ 0.04 (0.0022 yr⁻¹). The DIC increase is about 15% larger than expected from equilibrium with atmospheric CO₂. This could result from the increase between the two periods in the frequency and intensity of winter convection events. Likewise, it could be the signature of the contribution of the Atlantic Ocean as a source of anthropogenic carbon to the Mediterranean Sea through the strait of Gibraltar. Under this assumption, we estimate that the part of DIC accumulated over

32 the last 18 years represents ~30% of the total change of anthropogenic carbon since the
33 beginning of the industrial period.

34

35 **1 Introduction**

36 The concentration of atmospheric carbon dioxide (CO₂) has been increasing rapidly over the
37 20th century and, as a result, the concentration of dissolved inorganic carbon (DIC) in the near
38 surface ocean increases, which drives a decrease in pH in order to maintain a chemical
39 equilibrium [Millero, 2007]. These changes have complex direct and indirect impacts on
40 marine organisms and ecosystems [Gattuso and Hansson, 2011]. Empirical methods to
41 estimate the anthropogenic CO₂ penetration in the ocean since the industrial revolution have
42 improved over the past few decades [Chen and Millero, 1979; Gruber et al., 1996]; [Sabine et
43 al., 2008]; [Touratier and Goyet, 2004; 2009; Woosley et al., 2016]. As the concentration of
44 anthropogenic carbon, C_{ant}, cannot be distinguished from the natural background of DIC
45 through total DIC measurements, these methods are based on the analysis of different
46 chemical properties of the water column. Direct estimates of the anthropogenic CO₂
47 absorption in the sea surface layers are difficult owing to the large natural variability driven
48 by physical and biological phenomena. [Bates et al., 2014] have extracted the trend from the
49 large variability, based on analysis of a long time series (monthly or seasonal sampling). For
50 the global surface ocean, [Lauvset et al., 2015] have used the Surface Ocean CO₂ Atlas
51 (SOCAT) database [Bakker et al., 2014] combined with an interpolation method. Constraints
52 on the Mediterranean Sea's storage of anthropogenic CO₂ are limited, as the data based
53 approaches disagree by more than a factor of two [Huertas et al., 2009; Touratier and Goyet,
54 2009]. In addition to the anthropogenic signal, oceanic DIC can also be the signature of a
55 strong interannual variability. In the North Atlantic, for instance it has been shown that
56 because of decadal variability it requires 25 years for the long-term trend to emerge
57 [McKinley et al., 2011][McKinley et al., 2011][McKinley et al., 2011][McKinley et al., 2011].

58 A high frequency sampling of the seawater carbon chemistry at the air-water interface over
59 extended periods of time is a way to detect a possible trend in DIC. In this paper we analyze
60 two three-year time series of hourly fugacity of CO₂, fCO₂, measured with autonomous
61 CARIOCA sensors [Copin-Montégut et al., 2004; Merlivat and Brault, 1995] in 1995-1997
62 and 2013-2015, at two very close locations in the northwestern Mediterranean Sea (Fig. 1).
63 Using measured fCO₂, temperature (T) and salinity (S), we derive the other variables of the

64 carbonate system (pH and DIC). The experimental setting is first described, and the recent
65 data obtained over the 2013-2015 period are presented. Combined with the 1995-1997
66 measurements previously published [Hood and Merlivat, 2001], we estimate the decrease of
67 pH and the increase of DIC. The results are discussed with respect to the contributions of the
68 exchange with atmospheric CO₂, to the possible impact of vertical mixing and to recent
69 estimates of the transport of anthropogenic carbon from the Atlantic Ocean over a 18 years
70 period.

71

72 2 Material and methods

73 2.1-The BOUSSOLE and DYFAMED sites

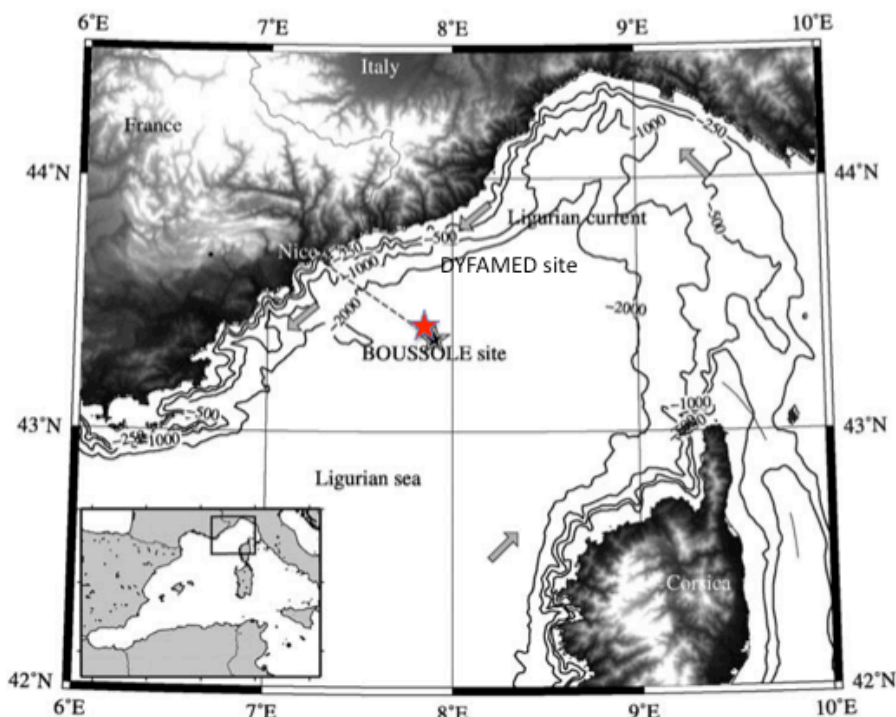


Fig. 1. The area of the northwestern Mediterranean Sea showing the southern coast of France, the island of Corsica, the main current branches (gray arrows), and the location of the DYFAMED site (red star) and the BOUSSOLE buoy (black star) in the Ligurian Sea.

74

75 Data collection was carried out at the BOUSSOLE site (43°22'N, 7°54'E) in 2013-2015
76 [Antoine *et al.*, 2008; Antoine. and others, 2006] and at the DYFAMED site (43°25'N,
77 7°52'E) in 1995-1997 [Marty *et al.*, 2002]. These sites are 3 nautical miles apart, both located
78 in the Ligurian Sea, one of the basins of the northwestern Mediterranean Sea (Fig.1). The
79 water depth is of ~2400 m. The prevailing ocean currents are usually weak (<20 cm s⁻¹),
80 because these sites are in the central area of the cyclonic circulation that characterizes the
81 Ligurian Sea. The two sites surrounded by the permanent geostrophic Ligurian frontal jet

82 flow are protected from coastal inputs [*Antoine et al.*, 2008; *Heimbürger et al.*, 2013; *Millot*,
83 1999]. Monthly cruises are carried out at the same location .

84

85 2.2- Analytical methods

86 At DYFAMED, fCO₂ measurements at 2 m depth were provided by an anchored floating
87 buoy fitted with a CARIOCA sensor. At BOUSSOLE, measurements were carried out from a
88 mooring normally dedicated to radiometry and optical measurements, and onto which two
89 CARIOCA sensors were installed. Both monitored fCO₂ hourly at 3 and 10 meters depth
90 (although only one of the two depths was equipped with a functional sensor at some periods);
91 S and T were monitored at the same two depths using a Seabird SBE 37-SM MicroCat
92 instrument. The CARIOCA sensors were adapted to work under pressure in the water column.
93 They were swapped about every 6 months, with serviced and calibrated instruments replacing
94 those having been previously deployed. The accuracy of CARIOCA fCO₂ measurements
95 using the spectrophotometric method with thymol blue is estimated at 2 µatm during both
96 periods. [*Hood and Merlivat*, 2001] have reported agreement between fCO₂ measured by
97 CARIOCA buoys, similar to the one deployed at DYFAMED, with ship based measurements,
98 during a number of field programs, with an accuracy of 2 µatm and a precision of 5 µatm .

99 At Boussole, newly designed fCO₂ sensors have been calibrated using in situ seawater
100 samples taken at 5 and 10 meters depth during the monthly servicing cruises to the mooring.
101 The samples were analyzed using potentiometric titration from the method developed by
102 [*Edmond*, 1970] with a closed cell, and provides measurements of DIC, and total alkalinity,
103 Alk. For calibration, Certified Reference Materials (CRMs) provided by Prof. A. Dickson
104 (Scripps Institution of Oceanography, San Diego, USA) were used. The accuracy is estimated
105 at 3 µmol kg⁻¹ for both DIC and Alk. fCO₂ is calculated using the dissociation constants of
106 Mehrbach refitted by Dickson and Millero [*Dickson and Millero*, 1987; *Mehrbach et al.*,
107 1973]. Error on fCO₂ derived from an individual sample is expected to be on the order of 5
108 µatm [*Millero*, 2007]. About 8 samples have been used to calibrate each CARIOCA sensor so
109 that the error on the absolute calibration of each fCO₂ CARIOCA sensor, is estimated at 1.8
110 µatm. In addition, we observe that the standard deviation of the difference between the
111 CARIOCA fCO₂ and fCO₂ computed with the monthly discrete samples (Fig. 2b) is equal to
112 4.4 µatm, consistent with the expected precision on CARIOCA fCO₂ of 5 µatm. Alk and S of
113 the 56 samples taken at BOUSSOLE are linearly correlated according the following
114 relationship :

$$115 \text{ Alk } (\mu\text{mol kg}^{-1}) = 87.647 \text{ S} - 785.5 \quad (1)$$

116 The standard deviation of the Alk data around the regression line is equal to $4.4 \mu\text{mol kg}^{-1}$
 117 ($r^2=0.89$).

118

119 3 Results

120 3.1 The BOUSSOLE mooring (2013-2015) time series

121 Temperature and $f\text{CO}_2$ were measured from February 2013 to February 2016. All seasons
 122 were well represented, with missing data only in May-July 2013. For some periods,
 123 simultaneous measurements were made at 3 and 10 m depth (Fig. 2, a, b, c).

124

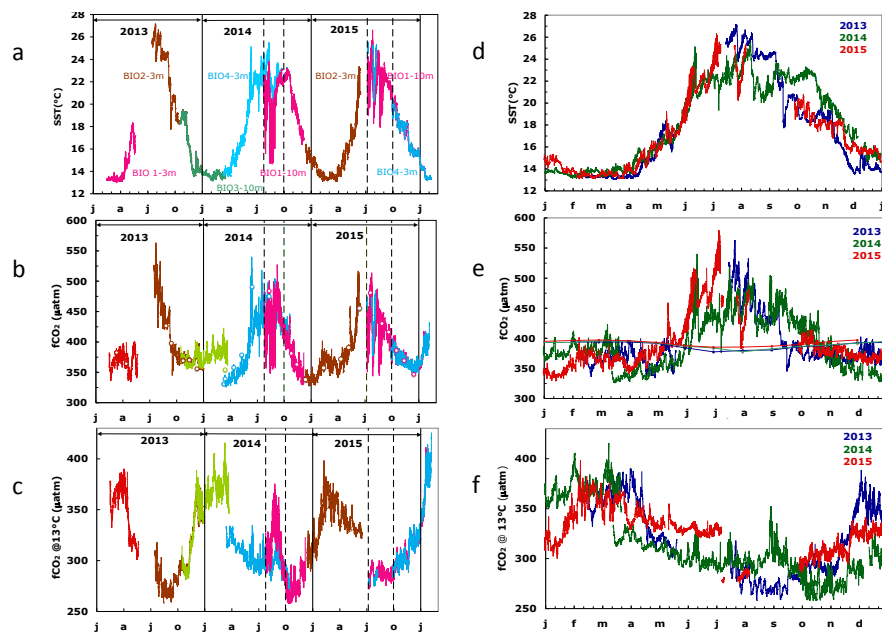


Fig. 2. Interannual variability of CARIOCA data: a) T, b) $f\text{CO}_2$, c) $f\text{CO}_2@13$. The dotted lines indicate the period affected by stratification and internal waves (July, 26th to October 1st, 2014 and July, 8th to October 1st, 2015). On 2(b), the open circles correspond to $f\text{CO}_2$ data derived from DIC and alkalinity measurements of samples taken at 5 and 10 meters. (d), (e), (f), seasonal variability. On 2(e), the thin lines indicate $f\text{CO}_{2\text{atm}}$. Note that the color code on (d), (e), (f) is different from (a), (b), (c).

125

126 The range of temperature (Fig. 2a) extends from 13°C in winter up to 27°C in summer,
 127 followed by progressive cooling in fall. The coldest temperature, 13°C , results from the
 128 winter vertical mixing with the deeper Levantine Intermediate Water, LIW, marked by
 129 extrema in temperature and salinity [Copin-Montegut and Begovic, 2002]. Temperature
 130 provides the main control of the seasonality of $f\text{CO}_2$, from $350 \mu\text{atm}$ to more than $550 \mu\text{atm}$ in
 131 summer 2013 (Fig. 2b). The fugacity of CO_2 in seawater is a function of temperature, DIC,
 132 alkalinity, salinity and dissolved nutrients. In the oligotrophic surface waters of the
 133 Mediterranean sea, this last effect should be negligible. Temperature and DIC have the
 134 strongest influences. By normalizing $f\text{CO}_2$ to a constant temperature, the thermodynamic

135 effect can be removed and changes in $f\text{CO}_2$ resulting from changes in DIC can be more easily
136 identified. Figure 2c shows the variability of $f\text{CO}_2$ normalized to the constant temperature of
137 13°C , ($f\text{CO}_2@13$), using the equation of [Takahashi *et al.*, 1993]. The underlying processes
138 that govern the seasonal variability of $f\text{CO}_2@13$ are successively winter mixing, biological
139 activity (organic matter formation and remineralization) and deepening of mixed layer in fall
140 [Begovic and Copin-Montegut, 2002; Hood and Merlivat, 2001]. Biology accounts for the
141 decline in $f\text{CO}_2@13$ observed from March-April to late summer; the ensuing increase of
142 surface $f\text{CO}_2@13$ is associated with the deepening of the mixed layer in the fall or convection
143 in winter as the vertical distribution of $f\text{CO}_2@13$ at DYFAMED shows a maximum in the 50-
144 150 m layer where a large remineralization of organic matter occurs, the productive layer
145 being mostly between 0 and 40 m [Copin-Montegut and Begovic, 2002]. The contribution of
146 air-sea exchange is not significant [Begovic and Copin-Montegut, 2002]. Over the period
147 2013-2015, the CO_2 air-sea flux from the atmosphere to the ocean surface is equal to -0.45
148 $\text{mmol m}^{-2} \text{yr}^{-1}$.

149 During summer 2014, large differences between measurements at 3 and 10 meters were
150 observed (Fig. 2, a, b, c between dashed lines). A detailed analysis of the temporal
151 variability during that period underscores the role of inertial waves at the frequency of
152 17.4 hours that create the observed differences between the 2 depths of observations,
153 the deeper waters being colder and enriched in $f\text{CO}_2@13$. T and $f\text{CO}_2@13$ variability is
154 dominated by inertial waves. In particular, from 15 to 26 of August 2014, the difference
155 in T between the two depths is as large as 7.6°C , and 5.1°C on average. $f\text{CO}_2$ decreases on
156 average by $32.7 \mu\text{atm}$ leading to an increase of $f\text{CO}_2@13$ equal to $42.8 \mu\text{atm}$.

157 The 2013-2015 seasonal and inter-annual variability of T, $f\text{CO}_2$ and $f\text{CO}_2@13$ is
158 illustrated on Fig. 2, d, e, f. The larger interannual changes in temperature (Fig.2, d) are
159 observed during summer, both at 3 m and 10 m depth, while over February and March, a
160 constant value of 13°C is observed as the result of vertical mixing with the LIW. A very
161 large inter-annual variability of $f\text{CO}_2@13$ is observed for $T < 14^\circ\text{C}$ (Fig. 2,f). This is
162 associated with the winter mixing at the mooring site, which is highly variable from year
163 to year. Winter mixed-layer depth, MLD, varies between 50 and 160 m, at the top of the
164 LIW over the 2013-2015 period [Coppola *et al.*, 2016]. The variable depth of the winter
165 vertical mixing causes the difference in $f\text{CO}_2@13$ as $f\text{CO}_2$ increases with depth [Copin-
166 Montegut and Begovic, 2002]. The deepening of MLD is driven by episodic and intense
167 mixing processes characterized by a succession of events lasting several days, related to

168 atmospheric forcing [Antoine et al., 2008] which lead to increase in $f\text{CO}_2@13$. Figure 2,e
169 illustrates the solubility control of the variability of $f\text{CO}_2$, as $f\text{CO}_2$ increases when T
170 increases. Another cause of inter-annual variability of $f\text{CO}_2$ for $T\sim 14^\circ\text{C}$ is the timing of
171 the spring increase of biological activity which differs by a month between years; for
172 instance, it happened at the beginning of April in 2013, $T\sim 15\text{-}16^\circ\text{C}$ and by mid March in
173 2014, $T\sim 14^\circ\text{C}$. Another cause is the deepening of the mixed layer due to the fall cooling
174 which varies by a month between years.

175

176 3.2 Decadal changes of hydrography

177 3.2.1 Sea surface temperature changes

178 Monthly mean values of temperature have been computed for the two three-year periods,
179 1995-1997 and 2013-2015. In 1995-1997, $f\text{CO}_2$ and T at 2 m were measured with CARIOCA
180 sensors installed on a buoy at DYFAMED [Hood and Merlivat, 2001]. The mean annual
181 temperature of hourly CARIOCA data is equal to 18.21°C . For 2013-2015, temperature
182 measurements made on the BOUSSOLE mooring at 3 and 10 meters have been used. For the
183 April to September time interval, there are only data at 3m depth. In addition, temperature
184 data measured half hourly at 0.7 m at a nearby meteorological buoy ($43^\circ 23' \text{N}$, $7^\circ 50' \text{E}$)
185 (<http://www.meteo.shom.fr/real-time/html/DYFAMED.html>) have been used (Fig.3d). Mean
186 annual temperature are equal to 18.29°C and 17.97°C respectively, based on the
187 meteorological buoy and the BOUSSOLE mooring data. The two sets of data differ
188 essentially during July and August, with the temperatures at 3 m being colder than at 0.7 m,
189 indicating a thermal gradient between the two depths during summer. Therefore, for 2013-
190 2015, we select the mean annual value computed with the meteorological buoy, 18.29°C , as
191 better representing the sea surface. This value is very close to 18.21°C computed for 1995-
192 1997. Then, no significant change of SST is found between the 2 decades, with a mean value
193 equal to 18.25°C .

194 3.2.2 Sea surface salinity changes

195 The mean value of salinity computed from 56 samples taken at BOUSSOLE in 2013-2015 is
196 equal to 38.19 ± 0.14 . In 1998-1999, ship measurements of surface salinity were made during
197 monthly cruises at the DYFAMED site [Copin-Montégut et al., 2004]. The mean salinity of
198 this set of 19 data is equal to 38.21 ± 0.12 . Thus, there is no significant salinity change
199 between the two decades.

200

201 3.3 Decadal changes of $f\text{CO}_2@13$

202 **3.3.1** Time series of $f\text{CO}_2@13$ in 1995-1997 and 2013-2015

203 The two time series of high frequency data were analyzed in order to quantify the change of
204 $f\text{CO}_2@13$ at the sea surface two decades apart. To account for the interannual seasonal
205 variability as well as irregular sampling, we performed an analysis of the change of $f\text{CO}_2@13$
206 as a function of SST (Fig. 3, a and b). For the 2013-2015 data set, we excluded summer data
207 measured at 10 m depth as they were not representative of the surface mixed layer due to a
208 strong stratification. Much larger $f\text{CO}_2@13$ values are observed at low temperature than at
209 high temperature, the decrease being similar for the two studied periods and strongly non
210 linear. As described in section 3.1, large values at low temperature result from mixing with
211 enriched deep waters during winter and low values for 26°C - 28°C temperatures occur at the
212 end of summer after biological drawdown of carbon. An increase of $f\text{CO}_2@13$ between the 2
213 periods is clearly highlighted for the whole range of temperature.

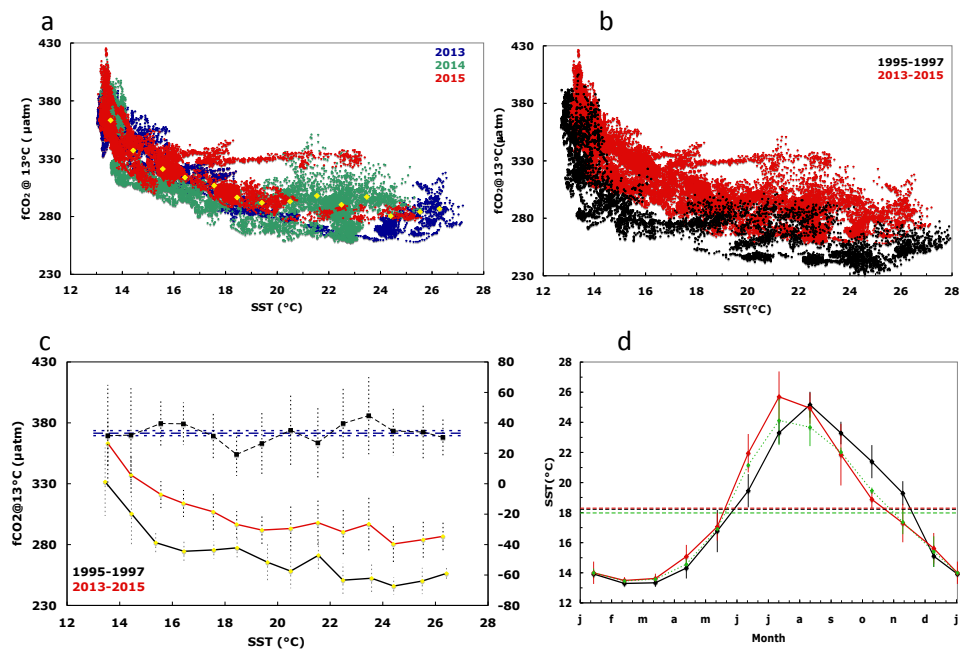


Fig.3. (a) $f\text{CO}_2@13^\circ\text{C}$ as a function of temperature for hourly data in 2013, 2014 and 2015. The yellow dots indicate mean $f\text{CO}_2@13^\circ\text{C}$ (b) as in (a) but for all hourly data in 1995-1997 (black) and in 2013-2015 (red) (c) As in (b), but for average values per 1°C interval (standard deviation as dotted line). The difference between the two periods is also displayed (dashed black curve; scale on the right axis). (d) Mean monthly sea surface temperature for 1993-1995 (black curve; CARIOCA sensors), 2013-2015 (green; CARIOCA sensors), 2013-2015 (red, meteorological buoy). Corresponding mean annual values are indicated by dotted lines.

214

215 **3.3.2** Trend analysis and statistics

216 To quantify the change of $f\text{CO}_2@13$ between the two data sets, we proceed as follows: data
217 are binned by 1°C temperature intervals, thereby removing any potential seasonal weighting,
218 especially towards the 13 - 14°C winter months temperature. The measurements made in this

219 temperature interval represent about 25% of the total number of data for both periods. For
 220 each of the fourteen 1°C step, the mean and standard deviation of hourly fCO₂@13
 221 measurements are reported in Table 1 and on Fig. 3c.
 222

Time interval 1995-1997				Time interval 2013-2015				Temporal trend	
T °C	fCO ₂ @13 µatm	N	standard deviation µatm	T °C	fCO ₂ @13 µatm	N	standard deviation µatm	dfCO ₂ @13 µatm	standard deviation µatm
13.45	331.58	1212	28.09	13.55	363.14	6869	18.07	31.56	33.40
14.45	305.28	495	26.02	14.43	337.16	3270	16.65	31.87	30.89
15.37	281.54	447	9.62	15.57	321.10	3112	11.09	39.56	14.68
16.44	274.43	182	8.53	16.42	313.79	1818	11.09	39.36	13.99
17.58	275.54	190	7.04	17.56	306.83	1528	14.65	31.29	16.25
18.47	277.34	300	9.04	18.45	296.57	2621	10.95	19.23	14.20
19.62	265.43	342	15.58	19.41	291.84	1406	13.45	26.40	20.59
20.50	258.08	529	14.15	20.50	293.16	1135	18.21	35.08	23.06
21.56	271.15	239	12.98	21.54	297.96	1200	20.41	26.82	24.19
22.49	250.75	742	13.66	22.49	290.27	2385	18.57	39.52	23.05
23.57	252.22	320	13.00	23.47	296.92	747	21.77	44.70	25.36
24.41	245.85	506	7.08	24.40	280.44	959	14.82	34.59	16.43
25.50	250.06	215	10.77	25.53	284.05	456	14.81	33.99	18.31
26.42	256.29	279	6.24	26.29	286.71	249	11.23	30.42	12.85

223

224

Table 1:

225 Distribution of temperature, fCO₂@13, and increase dfCO₂@13 data binned by 1°C
 226 temperature interval for the 2 periods 1995-1997 and 2013-2015 .

227 The mean temperature within each 1° step differ for the two periods as the distribution of
 228 individual measurements are not identical.

229 For both data sets, a monotonic relationship between fCO₂@13 and T is observed with
 230 correlation coefficients respectively equal to -0.861 and -0.857. The difference in fCO₂@13
 231 between the two periods, dfCO₂@13, is derived in each temperature step, as the difference

232 between column 2 and 6 of Table 1. The variability of this difference is estimated as the
 233 quadratic mean of the standard deviation in each time series. Both values are reported in
 234 Table 1, column 9 and 10, and on Fig. 3c.

235 It is interesting to note that the distribution of values around the mean seems random
 236 and indicates no trend dependency with SST (Fig. 3c). This suggests that the processes
 237 which control the seasonal variation of $f\text{CO}_2@13$ at the sea surface have not changed
 238 over the last two decades. The mean weighted value of $df\text{CO}_2@13$ over the whole range of
 239 temperature is estimated as the mean of $df\text{CO}_2@13$ in each temperature step weighted by the
 240 variance. It is equal to $32.7\mu\text{atm}$. We estimate the accuracy on this value as follows. For each
 241 time interval, the mean $f\text{CO}_2@13$ per temperature step has been derived from at least three
 242 independent CARIOCA sensors. Given that the accuracy on $f\text{CO}_2$ from each CARIOCA
 243 sensor is estimated at $2\mu\text{atm}$ and that the calibrations of the three sensors are independent,
 244 the accuracy on $f\text{CO}_2$ averaged in each time interval is $2/\sqrt{3}=1.15\mu\text{atm}$. Hence the accuracy
 245 on the difference is estimated at $1.6\mu\text{atm}$.

246

247 3.4 Changes of seawater carbonate chemistry in surface waters

248 We estimated the DIC and pH changes related to the increase of $f\text{CO}_2@13$ measured at the
 249 sea surface 18 years apart, assuming a mean salinity equal to 38.2, a mean alkalinity equal to
 250 $2562.3\mu\text{mol kg}^{-1}$ following equation (1), and a mean in situ temperature, T , equal to 18.25°C .
 251 The dissociation constants of Mehrbach refitted by Dickson and Millero [*Dickson and*
 252 *Millero, 1987; Mehrbach et al., 1973*] were used. pH is calculated on the seawater scale. We
 253 compute an increase of DIC, $d\text{DIC}$, equal to $24.8\pm 1.3\mu\text{mol kg}^{-1}$ ($1.38\pm 0.07\mu\text{mol kg}^{-1}\text{yr}^{-1}$)
 254 and the decrease of pH, $dp\text{H}$ equal to -0.0390 ± 0.0020 pH unit (-0.0022 ± 0.0001 pH unit^{yr}
 255 ¹) (Table 2).

	$d f\text{CO}_2^*$ @ 13°C μatm	$d f\text{CO}_2^*$ @ T μatm	$d \text{DIC}^*$ μmolkg^{-1}	$d \text{pH}^*$ pH unit	$df\text{CO}_2@T$ annual $\mu\text{atm yr}^{-1}$	$d \text{DIC}$ annual $\mu\text{molkg}^{-1}\text{yr}^{-1}$	$d \text{pH}$ annual pH unit yr^{-1}
sea surface	32.7 +/-1.6	40.8 +/-2.0	24.8 +/-1.3	-0.0390 +/-0.0020	2.27 +/-0.11	1.38 +/-0.07	-0.0022 +/-0.0001
atmosphere Lampedusa data		34.3 +/-1.2	**20.8 +/-0.8		1.91 +/-0.07		
$df\text{CO}_2@T_{\text{air}}/df\text{CO}_2@T_{\text{sea}}$		0.84 +/-0.05					

256

257 Table 2
258 Seasonally detrended long term and annual trends of seawater carbonate chemistry and
259 atmosphere composition.

260 T, mean annual temperature equal to 18.25°C

261 *, Change from 1995-1997 to 2013-2015.

262 **, $\Delta\text{DIC}_{\text{ant}}$

263

264 3.5 Changes in atmospheric and seawater fCO_2

265 The increase of atmospheric fCO_2 from 1995-1997 to 2013-2015 was computed from the
266 monthly atmospheric xCO_2 concentrations measured at the Lampedusa Island station (Italy)
267 ($35^{\circ}31'N$, $12^{\circ}37'E$) (<http://ds.data.jma.go.jp/gmd/wdcgg/>) (see equation 3 in [Hood and
268 *Merlivat*, 2001]). Considering a mean annual in situ temperature equal to 18.25°C and an
269 atmospheric pressure equal to 1 atm, we derived a mean atmospheric fCO_2 equal to $355.3 \pm$
270 $0.8 \mu\text{atm}$ and $389.6 \pm 0.9 \mu\text{atm}$ for 1995-1997 and 2013-2015, that is an increase equal to
271 $34.3 \pm 1.2 \mu\text{atm}$ (Table 2). At this temperature, the change of fCO_2 at the sea surface is equal
272 to $40.8 \pm 2.0 \mu\text{atm}$. Thus the contribution of the increase in atmospheric CO_2 is responsible
273 for $84 \pm 5\%$ of the increase of fCO_2 measured in the surface waters. Assuming the same
274 salinity and alkalinity as previously, the corresponding amount of anthropogenic carbon taken
275 up from the atmosphere in order to maintain a chemical equilibrium at the sea surface would
276 be equal to $20.8 \pm 0.8 \mu\text{mol kg}^{-1}$ (Table 2).

277

278 4 Discussion

279 4.1 fCO_2 at the air-sea interface

280 We have computed that 84% of the increase of $\text{fCO}_2_{\text{sea}}$ in the northwestern Mediterranean,
281 two decades apart, comes from the atmosphere. One implicit assumption is that any change in
282 atmospheric fCO_2 immediately transfers as a change in the surface ocean fCO_2 . In agreement
283 with the circulation pattern of the basin [Millot, 1999], this increase of surface fCO_2 could
284 follow two routes: in situ chemical equilibrium at the air-sea interface or winter mixing with
285 DIC rich Levantine Intermediate water or surface waters of Atlantic origin, relatively
286 enriched in anthropogenic carbon. Keeping in mind that the deep-water renewal time is
287 estimated to be 20-40 years in the western basin, and given that the atmospheric increase was
288 slower 20-40 years ago, our estimate of the atmospheric contribution to the ocean trend is
289 likely an upper bound.

290 The mean values of fCO_2 computed at the mean annual SST, 18.25°C, computed with all the

291 individual hourly $f\text{CO}_2$ measurements in 1995-1997 and 2013-2015 are respectively equal to
292 352.3 μatm and 400.2 μatm , while the corresponding atmospheric values are 355.3 μatm and
293 389.6 μatm respectively. The CO_2 annual flux is directed from the atmosphere to the sea in
294 both cases, although the annual average of $f\text{CO}_2$ in surface seawater in 2013-2015 is higher
295 than atmospheric $f\text{CO}_2$. This is due to higher wind speed in autumn and winter when the
296 surface water is undersaturated (Fig.2, b).

297

298 4.2 Time change of surface alkalinity?

299 In the range of salinity of the BOUSSOLE samples, 37.9 to 38.5 psu, the alkalinity values
300 computed with Eq (1) are larger than those predicted by the [Copin-Montegut and Begovic,
301 2002] relationship established for the DYFAMED site, with a mean difference equal to $10\pm$
302 $2 \mu\text{mol kg}^{-1}$. In both cases alkalinity measurements were made with a potentiometric method
303 using certified reference material supplied by AG Dickson for calibration.

304 It is difficult to identify the cause for a possible change of alkalinity between the 2 periods, 18
305 years apart, while no salinity change has been observed. At a coastal site 50 km away from
306 DYFAMED, [Kapsenberg *et al.*, 2017] have measured an increase of alkalinity unrelated to
307 salinity over the period from 2007 to 2015. They attribute it to changes in freshwater inputs
308 from land. However, based on data from Coppola *et al.*, [2016], alkalinity in the upper 50m at
309 DYFAMED did not change significantly from 2007 through 2014 ($3.204 \mu\text{mol kg}^{-1}$,
310 $P=0.0794$, $r^{*2}=0.08$). Thus, we cannot conclude on whether the difference observed at
311 DYFAMED/BOUSSOLE between the two periods is real or an artifact of measurement
312 techniques. However, as a sensitivity test, if we compute the expected changes of DIC and pH
313 from 1995-1997 to 2013-2015 for a mean alkalinity increase of $10 \mu\text{mol kg}^{-1}$, we get annual
314 changes, $d\text{DIC}=+0.46 \mu\text{mol kg}^{-1}\text{yr}^{-1}$ and $d\text{pH}=-0.0001 \text{ pH unit yr}^{-1}$. Such a change in
315 alkalinity does not significantly affect the decrease of pH shown in Table 2.

316

317 4.3 Anthropogenic carbon storage in surface waters

318 The increase of sea surface DIC from 1995-1997 to 2013-2015 is equal to $24.8\pm 1.3 \mu\text{mol}$
319 kg^{-1} (Table 2). ($d\text{DIC}_{\text{ant}}$) predicted solely from chemical equilibrium of the sea surface with
320 the atmosphere is equal to $20.8\pm 0.8 \mu\text{mol kg}^{-1}$. The ratio of these two terms is equal to
321 0.84 ± 0.05 . In order to interpret the additional contribution of DIC to that resulting from the
322 local CO_2 air-sea exchange, we examine below two processes, respectively an increased
323 mixing with deep waters and an anthropogenic carbon invasion.

324 MLD time series show a strong variability in winter at interannual scale. During the two
325 periods, 1995-1997 and 2013-2015, the winter MLD never exceeded 220 m, whereas values
326 over 300 m were observed in 1999 and especially in February and March 2006 with values
327 close to 2000 m [Coppola et al., 2016; Pasqueron de Fommervault et al., 2015]. These
328 episodes of strong and deep vertical mixing must have entrained DIC rich LIW in the surface
329 waters. This could be a cause for the observed increase of DIC measured between the two
330 periods 1995 -1997 and 2013-2015.

331 As a result of a monitoring program in the Strait of Gibraltar, [Huertas et al., 2009]
332 calculated a net flux of C_{ant} from the Atlantic towards the Mediterranean basin. [Schneider et
333 al., 2010], using the transit time distribution method applied to a dataset from a cruise in the
334 Mediterranean Sea in 2001, estimated that the input of C_{ant} through the Strait of Gibraltar
335 from 1850 to 2001 accounts for almost 10% of the total C_{ant} inventory of the Mediterranean
336 Sea, which means that ~90% must have been taken up directly from the atmosphere. Based on
337 a high-resolution regional model, [Palmiéri et al., 2015] computed the anthropogenic carbon
338 storage in the Mediterranean basin. They concluded that 75% of the total storage of C_{ant} in the
339 whole basin comes from the atmosphere and 25% from net transport from the Atlantic across
340 the Strait of Gibraltar. The findings of these two studies support the conclusion that computed
341 change of DIC in excess of 16+/-5% over the direct contribution of air-sea exchange could
342 result from the anthropogenic carbon input from the Atlantic Ocean towards the
343 Mediterranean basin. [Huertas et al., 2009] and [Schneider et al., 2010] report DIC_{ant} surface
344 concentrations respectively equal to 65-70 $\mu\text{mol kg}^{-1}$ at the strait of Gibraltar in the years
345 2005-2007 and close to 65 $\mu\text{mol kg}^{-1}$ in the western basin in 2001. We extrapolate these
346 figures to the year 2014, assuming a mean increase rate of DIC equal to 1.38 $\mu\text{mol kg}^{-1}\text{yr}^{-1}$ as
347 previously computed (Table 2). Taking into account the increase of DIC_{ant} equal to 24.8 μmol
348 kg^{-1} between 1995-1997 and 2013-2015, we would estimate that the contribution of the
349 change of DIC_{ant} over the last 18 years represents ~30% of the total change since the
350 beginning of the industrial period ($t > \sim 1800$).

351

352 4.4 The signal of acidification

353 The annual decrease of pH_T calculated between 1995-1997 and 2013-2015 is equal to -
354 0.0022+/-0.0001. At the DYFAMED site, at 10 m depth, [Marcellin Yao et al., 2016] studied
355 the time variability of pH over 1995-2011, based on measurements of T, S, Alk and DIC
356 sampled approximately once a month. They computed a mean annual decrease of $-0.003 \pm$
357 0.001 pH units on the seawater scale that is not significantly different from our estimate.

358 [Bates *et al.*, 2014] examined changes in surface seawater CO₂-carbonate chemistry at the
359 locations of seven ocean CO₂ time series that have been gathering sustained observations
360 from 15 to 30 years with monthly or seasonal sampling. The range of decreasing trends of pH
361 extends from -0.0026±0.0006 unit yr⁻¹ at the Irminger Sea time series site to -0.0014±
362 0.0005 unit yr⁻¹ at the Iceland Sea time series. For the global surface ocean, [Lauvset *et al.*,
363 2015] have reported a mean rate of decrease of -0.0018±0.0004 for 1991-2011. The decrease
364 of pH computed here at DYFAMED is in the upper range of values compared to other time
365 series. The Mediterranean Sea is actually able to absorb more anthropogenic CO₂ per unit
366 area, first because of its higher total alkalinity that leads to a greater chemical capacity to take
367 up anthropogenic CO₂ and, second, because deep waters are ventilated on relatively short
368 timescales (30-40 years in the western basin), which allows deeper penetration of
369 anthropogenic tracers [Schneider *et al.*, 2010], [Palmiéri *et al.*, 2015]. The lowering effect of
370 high alkalinity on the Revelle factor, close to ten, implies a relatively high uptake capacity for
371 anthropogenic carbon, C_{ant}.

372

373 **5 Conclusion**

374 High-frequency ocean fCO₂ measurements made by CARIOCA sensors were sufficient to
375 estimate trends in fCO₂, DIC and pH over a period of two decades, notwithstanding a
376 considerable short-time and natural seasonal variability of these properties at the sea surface.
377 We have estimated a large change of sea surface carbonate chemistry, an increase of DIC and
378 a decrease of pH. The computed increase of DIC is larger than the change expected from
379 chemical equilibrium with atmospheric CO₂. This could be the result of a strong interannual
380 variability of the winter mixing as observed between the two periods 1993-1995 and 2013-
381 2015. Likewise, our results support modeling work and analysis of vertical profiles
382 measurements that suggest that the Atlantic Ocean contributes as a source of anthropogenic
383 carbon towards the Mediterranean basin, close to 10% ([Schneider *et al.*, 2010] or 25%
384 [Palmiéri *et al.*, 2015]).

385

386 *Data availability:* Time series data from Dyfamed (1995-1997) are available in the SOCAT v3
387 database. Boussole data (2013-2015) will be available in SOCAT v6.

388

389 **Acknowledgments**

390 Seawater samples were analyzed for DIC and Alk by the SNAPO-CO₂ at LOCEAN in Paris.
391 The CO₂Sys toolbox of [Pierrot *et al.*, 2006] has been used for the calculations of DIC and

392 pH. The adaptation of CARIOCA sensors to high pressure has been supported by the BIO-
393 optics and CARbon EXperiment (BIOCAREX) project, funded by the Agence Nationale de la
394 Recherche (ANR,Paris). We are grateful for helpful comments from Gilles Reverdin on the
395 manuscript. Many thanks to Laurent Coppola who kindly provided additional MLD data at
396 Dyfamed.

397

398 **References**

399

400 Antoine, D., F. d'Ortenzio, S. B. Hooker, G. Bécu, B. Gentili, D. Tailliez, and A. J. Scott
401 (2008), Assessment of uncertainty in the ocean reflectance determined by three satellite
402 ocean color sensors (MERIS, SeaWiFS and MODIS-A) at an offshore site in the
403 Mediterranean Sea (BOUSSOLE project), *Journal of Geophysical Research*, 113(C7).

404 Antoine., and others (2006), BOUSSOLE: A Joint CNRS-INSU,ESA, CNES and NASA ocean
405 color calibration and validation activity., *NASA Tech. Memo. 2006-214147*.

406 Bakker, D. C. E., et al. (2014), An update to the Surface Ocean CO₂ Atlas
407 (SOCAT version 2), *Earth Syst. Sci. Data*, 6(1), 69-90.

408 Bates, N., Y. Astor, M. Church, K. Currie, J. Dore, M. Gonaález-Dávila, L. Lorenzoni, F.
409 Muller-Karger, J. Olafsson, and M. Santa-Casiano (2014), A Time-Series View of Changing
410 Ocean Chemistry Due to Ocean Uptake of Anthropogenic CO₂ and Ocean Acidification,
411 *Oceanography*, 27(1), 126-141.

412 Begovic , M., and C. Copin-Montegut (2002), Processes controlling annual variations in
413 the partial pressure of fCO₂ in surface waters of the central northwestern
414 Mediterranean sea (Dyfamed site), *Deep-Sea Research II*, 49, 2031-2047.

415 Chen, G. T., and F. J. Millero (1979), Gradual increase of oceanic CO₂, *Nature*, 277, 205-
416 206.

417 Copin-Montegut, C., and M. Begovic (2002), Distributions of carbonate properties and
418 oxygen along the water column (0–2000 m) in the central part of the NW Mediterranean
419 Sea (Dyfamed site): influence of winter vertical mixing on air–sea CO₂ and O₂
420 exchanges, *Deep-Sea Research II* 49, 2049-2066.

421 Copin-Montégut, C., M. Bégovic, and L. Merlivat (2004), Variability of the partial pressure
422 of CO₂ on diel to annual time scales in the Northwestern Mediterranean Sea, *Mar Chem*,
423 85(3-4), 169-189.

424 Coppola, L., E. Diamond Riquier, and T. Carval (2016), Dyfamed observatory data,
425 *SEANOE*.

426 Dickson, A. G., and F. J. Millero (1987), A comparison of the equilibrium constants for the
427 dissociation of carbonic acid in seawater media, *Deep Sea Research Part A*.
428 *Oceanographic Research Papers*, 34(10), 1733-1743.

429 Edmond, J. M. (1970), High precision determination of titration alkalinity and total
430 carbon dioxide content of seawater by potentiometric titration, *Deep Sea research* 17(4),
431 737-750.

432 Gattuso, J.-P., and L. Hansson (2011), Ocean Acidification, *Oxford University Press*, 352
433 pp.

434 Gruber, N., J. L. Sarmiento, and T. F. Stocker (1996), An improved method for detecting
435 anthropogenic CO₂ in the oceans, *Global Biogeochem Cy*, 10, 809-837.

436 Heimbürger, L.-E., H. Lavigne, C. Migon, F. D'Ortenzio, C. Estournel, L. Coppola, and J.-C.
437 Miquel (2013), Temporal variability of vertical export flux at the DYFAMED time-series
438 station (Northwestern Mediterranean Sea), *Progress In Oceanography*, 119, 59-67.

439 Hood, E. M., and L. Merlivat (2001), Annual and interannual variations of fCO₂ in the
440 northwestern Mediterranean Sea: Results from hourly measurements made by CARIOCA
441 buoys, 1995-1997, *J Mar Res*, 59, 113-131.

442 Huertas, I. E., A. F. Ríos, J. García-Lafuente, A. Makaoui, S. ` Rodríguez-Gálvez, A. Sánchez-
443 Román, A. Orbi, J. Ruíz, and F. F. and Pérez (2009), Anthropogenic and natural CO₂
444 exchange through the Strait of Gibraltar, *Biogeosciences*, 6, 647-662.

445 Kapsenberg, L., S. Alliouane, F. Gazeau, L. Mousseau, and J.-P. Gattuso (2017), Coastal
446 ocean acidification and increasing total alkalinity in the northwestern Mediterranean
447 Sea, *Ocean Science*, 13(3), 411-426.

448 Lauvset, S. K., N. Gruber, P. Landschützer, A. Olsen, and J. Tjiputra (2015), Trends and
449 drivers in global surface ocean pH over the past 3 decades, *Biogeosciences*, 12(5), 1285-
450 1298.

451 Marcellin Yao, K., O. Marcou, C. Goyet, V. Guglielmi, F. Touratier, and J.-P. Savy (2016),
452 Time variability of the north-western Mediterranean Sea pH over 1995-2011, *Marine*
453 *Environmental Research*, 116, 51-60.

454 Marty, J. C., J. Chiaverini, M. Pizay, D., and B. Avril (2002), Seasonal and interannual
455 dynamics of nutrients and phytoplankton pigments in the western Mediterranean Sea at
456 the DYFAMED time-series station (1991-1999), *Deep-Sea Research II*, 49, 1965-1985.

457 McKinley, G. A., A. R. Fay, T. Takahashi , and N. Metzl (2011), Convergence of
458 atmospheric and North Atlantic carbon dioxide trends on multidecadal timescales,
459 *Nature Geoscience*, 4, 606-610.

460 Mehrbach, C., C. H. Culberson, J. E. Hawley, and R. M. Pytkowicz (1973), Measurement of
461 the apparent dissociation constants of carbonic acid in seawater at atmospheric
462 pressure, *Limnol Oceanogr*, 18(6), 897-907.

463 Merlivat, L., and P. Brault (1995), CARIOCA BUOY: Carbon Dioxide Monitor, *Sea*
464 *Technol*(October), 23-30.

465 Millero, F. J. (2007), The marine inorganic carbon cycle, *Chemical reviews*, 107(2), 308-
466 341.

467 Millot (1999), Circulation in the Western Mediterranean Sea, *Journal of Marine Systems*,
468 20, 423-442.

469 Palmiéri, J., J. C. Orr, J. C. Dutay, K. Béranger, A. Schneider, J. Beuvier, and S. Somot
470 (2015), Simulated anthropogenic CO₂ storage and acidification of the Mediterranean
471 Sea, *Biogeosciences*, 12(3), 781-802.

472 Pasqueron de Fommervault, O., C. Migon, F. D'Ortenzio, M. Ribera d'Alcalà, and L.
473 Coppola (2015), Temporal variability of nutrient concentrations in the northwestern
474 Mediterranean sea (DYFAMED time-series station), *Deep Sea Research Part I:*
475 *Oceanographic Research Papers*, 100, 1-12.

476 Pierrot, D., E. Lewis, and D. W. R. Wallace (2006), MS excel program developed for CO₂
477 system calculations, *In: Carbon Dioxide Information Analysis Center (ed.O.R.N.L.).*
478 *US.Department of Energy, Oak Ridge, TN.*

479 Sabine, C. L., R. A. Feely, F. J. Millero, A. G. Dickson, C. Langdon, S. Mecking, and D. Greeley
480 (2008), Decadal changes in Pacific carbon, *J.Geophys.Res.*, 113(C07021).

481 Schneider, A., T. Tanhua, A. Körtzinger, and D. W. R. Wallace (2010), High anthropogenic
482 carbon content in the eastern Mediterranean, *Journal of Geophysical Research*, 115(C12).

483 Takahashi , T., J. Olafson, J. G. Goddard, D. W. Chipman , and G. Sutherland (1993),
484 Seasonal variations of CO₂ and nutrients in the high-latitude surface oceans:a
485 comparative study, *Global Biogeochem Cy*, 7(4), 843-878.

486 Touratier, F., and C. Goyet (2004), Applying the new TrOCA approach to assess the
487 distribution of anthropogenic CO₂ in the Atlantic Ocean, *Journal of Marine Systems*, 46(1-
488 4), 181-197.

489 Touratier, F., and C. Goyet (2009), Decadal evolution of anthropogenic CO₂ in the
490 northwestern Mediterranean Sea from the mid-1990s to the mid-2000s, *Deep Sea*
491 *Research Part I: Oceanographic Research Papers*, 56(10), 1708-1716.

492 Woosley, R. J., F. J. Millero, and R. Wanninkhof (2016), Rapid anthropogenic changes in
493 CO₂ and pH in the Atlantic Ocean: 2003-2014, *Global Biogeochem Cy*, 30(1), 70-90.

494

495

496

496

Figure caption and tables

497 Figure 1. The area of the northwestern Mediterranean Sea showing the southern coast of
498 France, the Island of Corsica, the main current branches (gray arrows), and the location of the
499 DYFAMED site (43°25'N, 7°52'E, red star) and the BOUSSOLE buoy (43°22'N, 7°54'E,
500 black star) in the Ligurian Sea.

501

502 Figure 2. Interannual variability of CARIOCA data: a) T, b) fCO₂, c) fCO₂@13. The dotted
503 lines indicate the period affected by stratification and internal waves (July, 26th to October
504 1st, 2014 and July, 8th to October 1st, 2015). On 2(b), the open circles correspond to fCO₂
505 data derived from DIC and alkalinity measurements of samples taken at 5 and 10 meters. (d),
506 (e), (f), seasonal variability. On 2(e), the thin lines indicate fCO_{2atm}. Note that the color code
507 on (d), (e), (f) is different from (a), (b), (c).

508

509 Figure 3. (a) fCO₂@13 as a function of temperature for hourly data in 2013, 2014 and
510 2015. The yellow dots indicate mean fCO₂@13 (b) as in (a) but for all hourly data in 1995-
511 1997 (black) and in 2013-2015 (red) (c) As in (b), but for average values per 1°C interval
512 (standard deviation as dotted line). The difference between the two periods is also displayed
513 (dashed black curve; scale on the right axis). (d) Mean monthly sea surface temperature for
514 1993-1995 (black curve; CARIOCA sensors), 2013-2015 (green; CARIOCA sensors), 2013-
515 2015 (red, meteorological buoy). Corresponding mean annual values are indicated by dotted
516 lines.

517

518 Table 1:

519 Distribution of temperature, fCO₂@13, and increase dfCO₂@13 data binned by 1°C
520 temperature interval for the 2 periods 1995-1997 and 2013-2015 .

521 The mean temperature within each 1° step differ for the two periods as the distribution of
522 individual measurements are not identical.

523

524 Table 2

525 Seasonally detrended long term and annual trends of seawater carbonate chemistry and
526 atmosphere composition.

527 T, mean annual temperature equal to 18.25°C

528 *, Change from 1995-1997 to 2013-2015.

529 **, dDIC_{ant}